Electronic Supplementary Material (ESI) for Journal of Materials Chemistry A.
This journal is © The Royal Society of Chemistry 2022

Electronic Supplementary Information

Coupling Novel Li_7TaO_6 Surface Buffering with Bulk Ta-Doping to Achieve Long-Life Sulfide-Based All-Solid-State Lithium Batteries

Jie Shi[a], Zhihui Ma[a], Kun Han[a], Qi Wan[b], Di Wu[a], Xuanhui Qu[a], Ping Li[a]*

[a] Beijing Advanced Innovation Center for Materials Genome Engineering, Institute for Advanced Materials and Technology, University of Science and Technology Beijing, Beijing 100083, PR China.

[b] School of Materials and Chemistry, Southwest University of Science and Technology, Mianyang, Sichuan 621010, PR China.

* Corresponding author.

E-mail address: ustbliping@126.com.

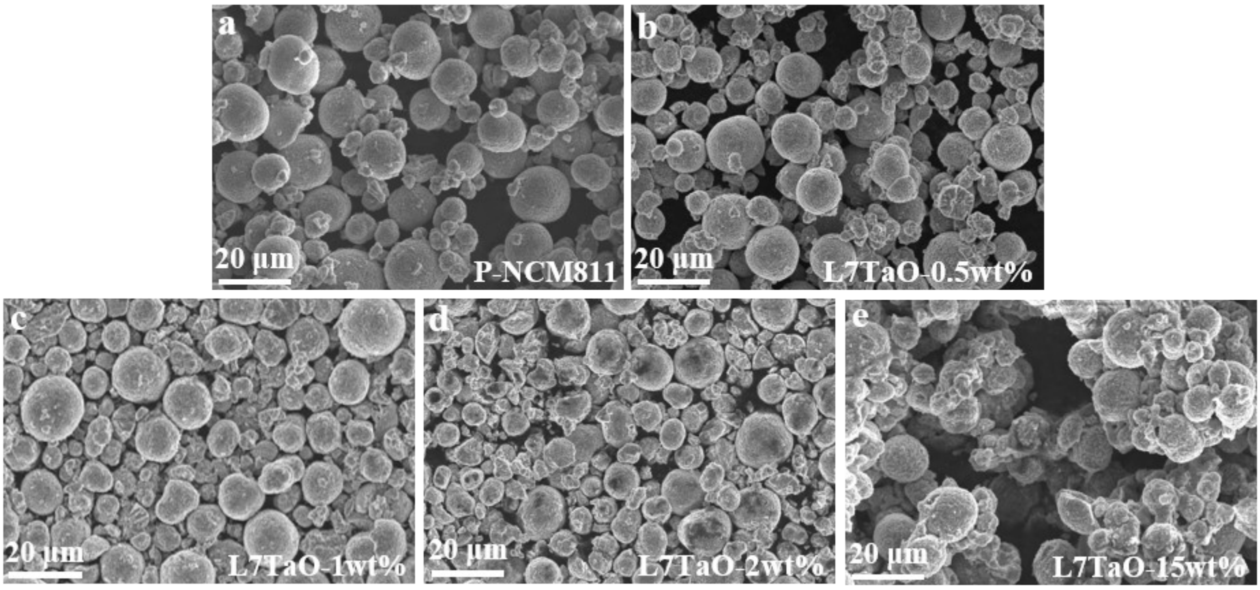

Fig. S1. SEM images of (a) P-NCM811, (b) L7TaO-0.5 wt%, (c) L7TaO-1 wt%, (d) L7TaO-2 wt% and (e) L7TaO-15 wt%.

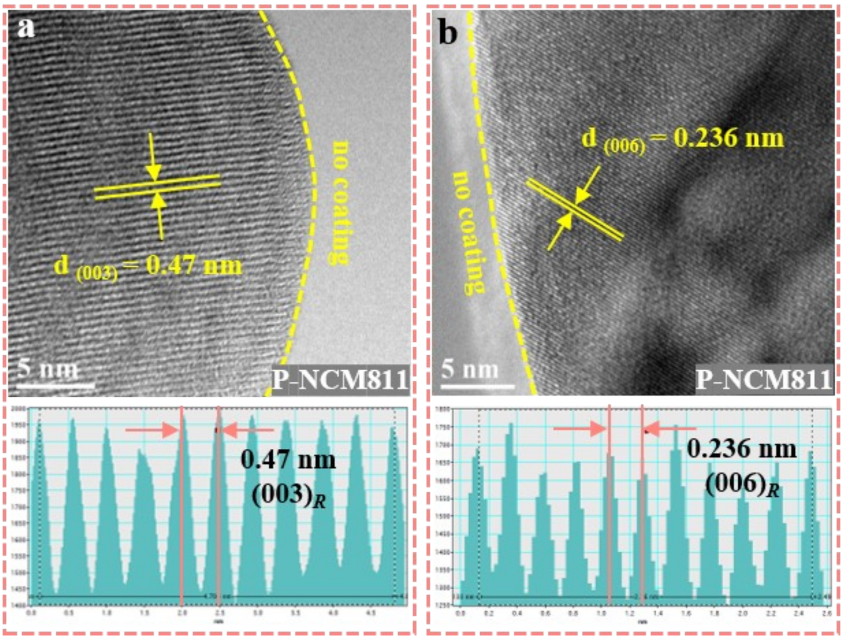

Fig. S2. HRTEM images of (a, b) P-NCM811 at different regions.

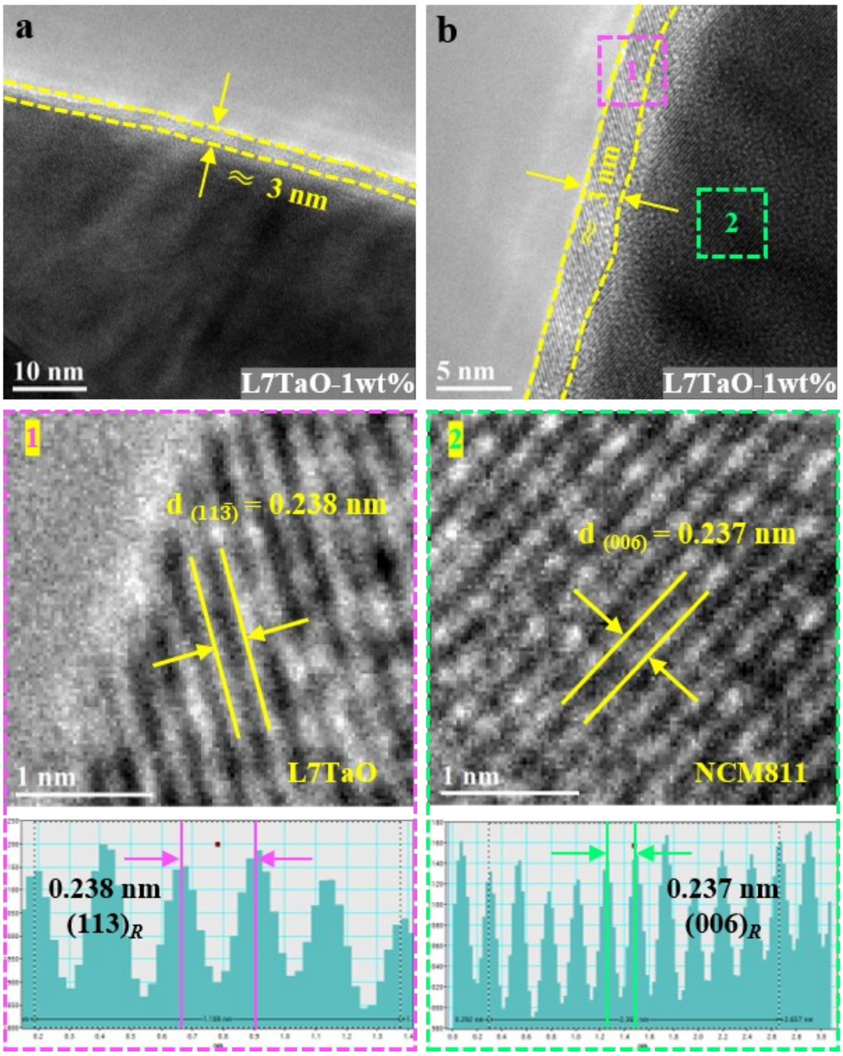

Fig. S3. HRTEM images of (a, b) L7TaO-1 wt% at different regions (Images of 1 and 2 correspond to the position 1,2 of (b)). The distance of the two yellow dotted lines represents the thickness of the buffering layer.

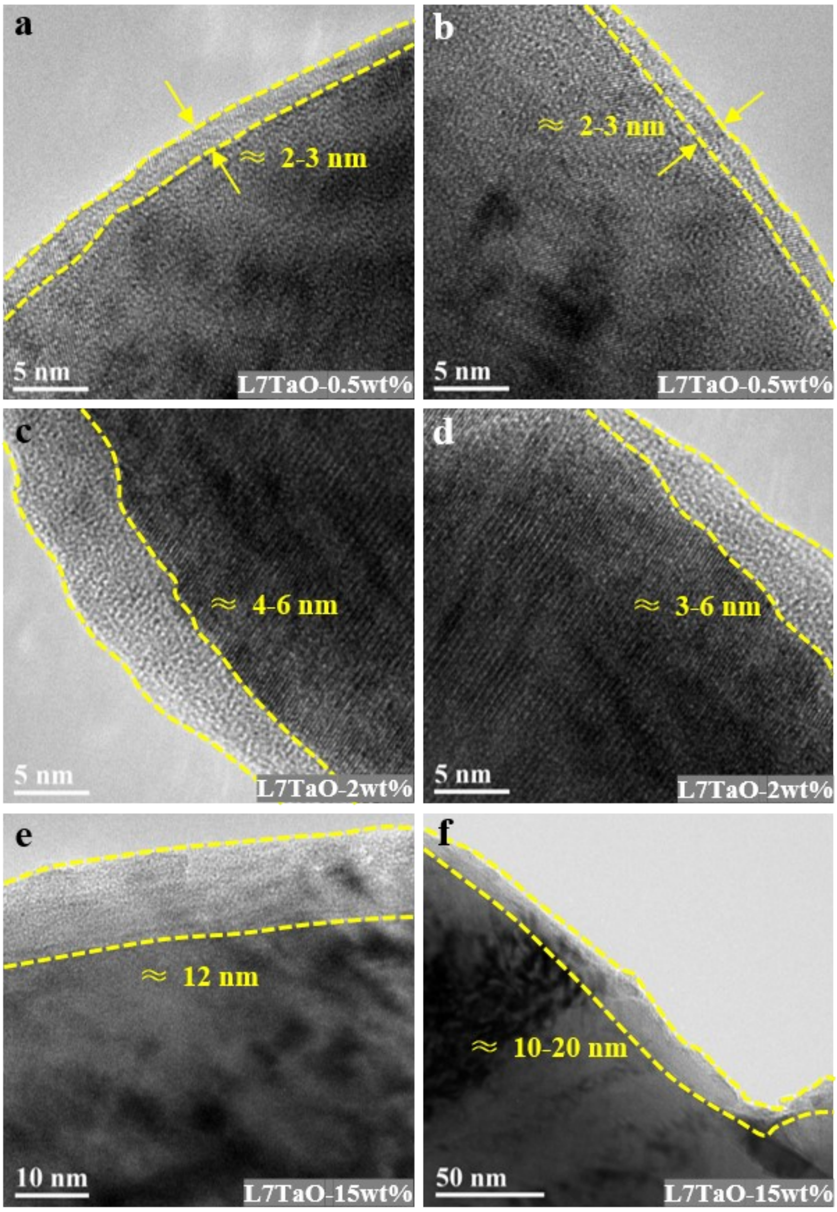

Fig. S4. HRTEM images of (a, b) L7TaO-0.5 wt%, (c, d) L7TaO-2 wt% and (e, f) L7TaO-15 wt% at different regions. The distance of the two yellow dotted lines represents the thickness of the buffering layer.

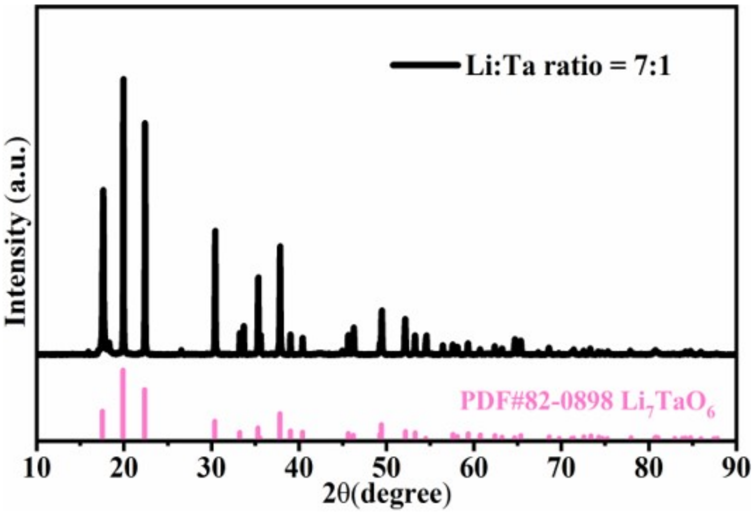

Fig. S5. The XRD patterns of obtained Li_7TaO_6.

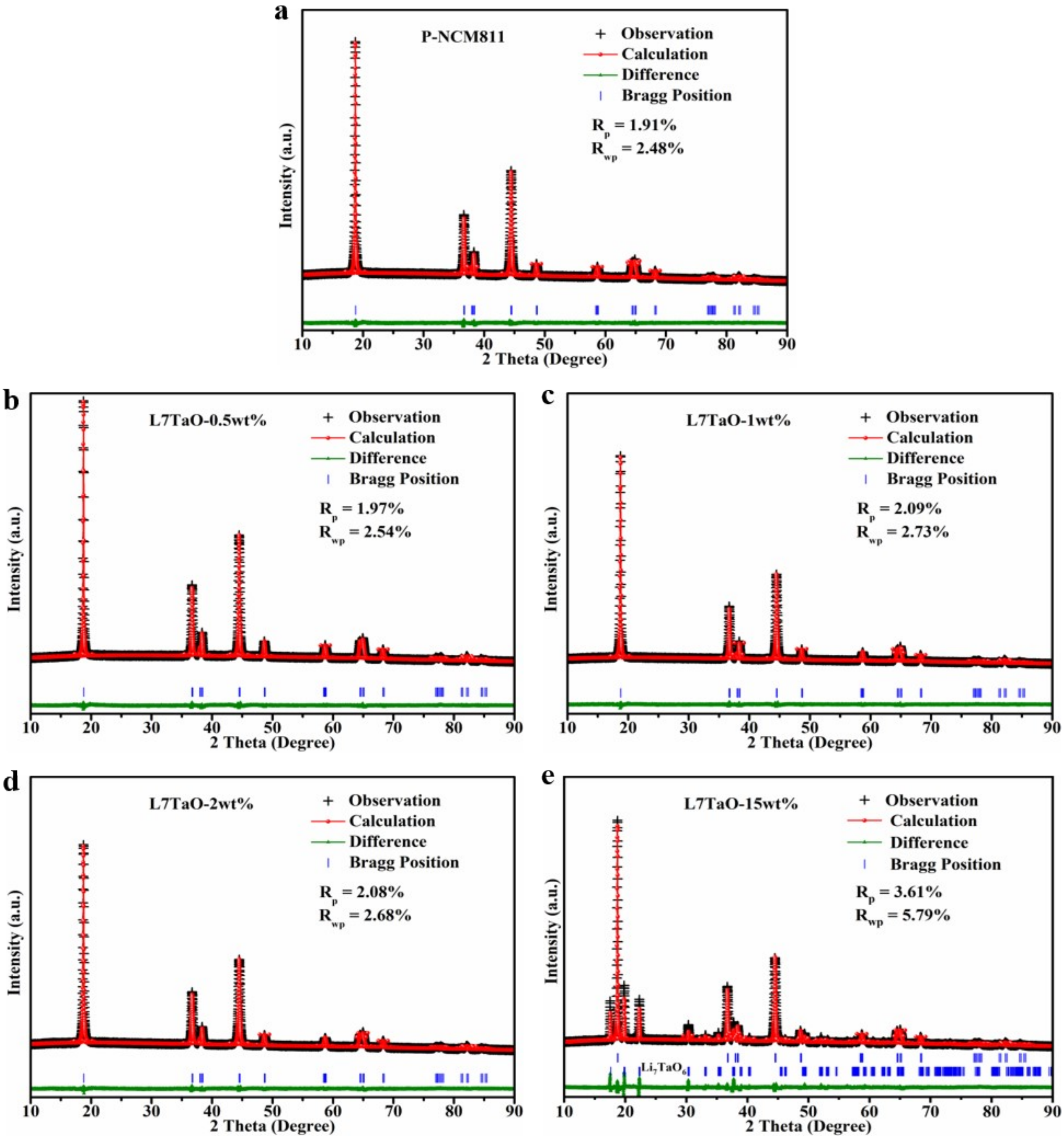

Fig. S6. XRD patterns and Rietveld analysis of (a) P-NCM811, (b) L7TaO-0.5 wt%, (c) L7TaO-1 wt%, (d) L7TaO-2 wt% and (e) L7TaO-15 wt% materials.

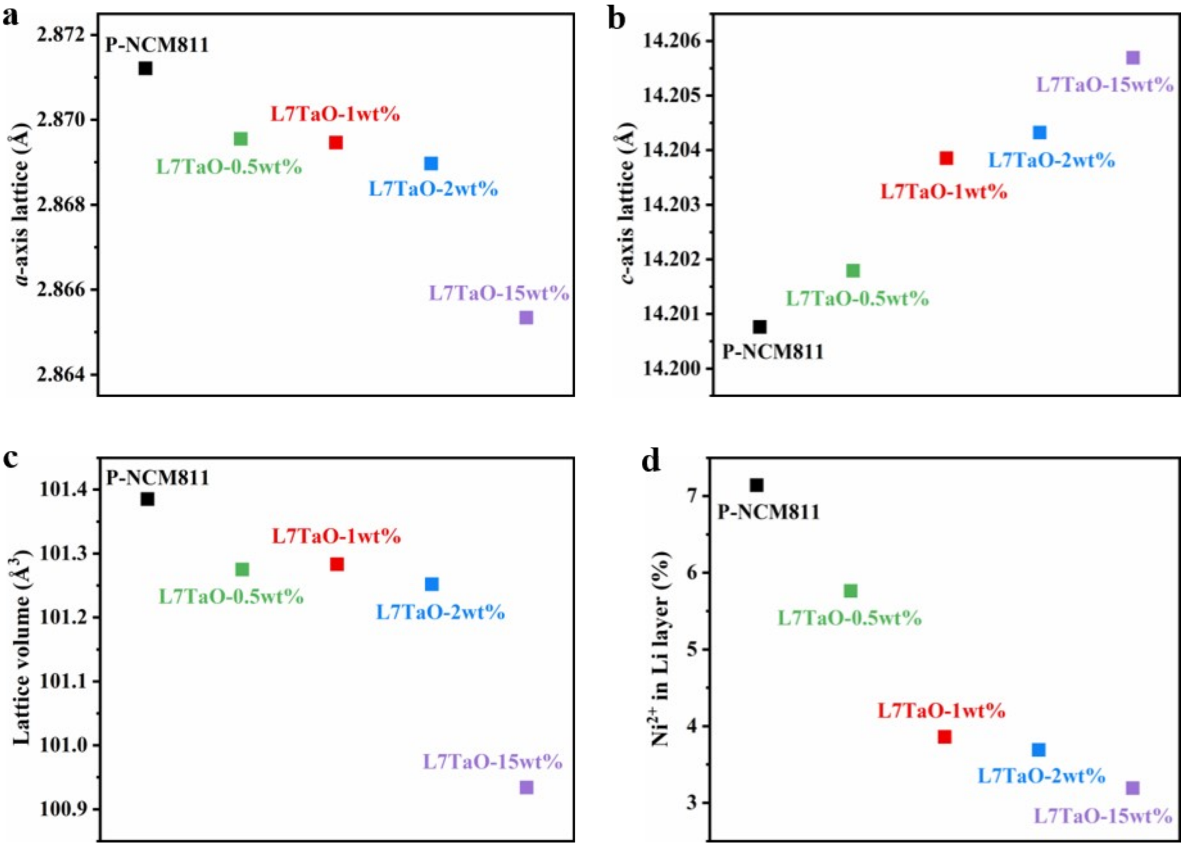

Fig. S7. The evolutions of XRD Rietveld refinement data for P-NCM811 and L7TaO-Q wt% (Q = 0.5, 1, 2 and 15) materials: (a) lattice parameters *a*, (b) lattice parameters *c*, (c) lattice parameters *V* and (d) the Li^+/Ni^{2+} mixing degree.

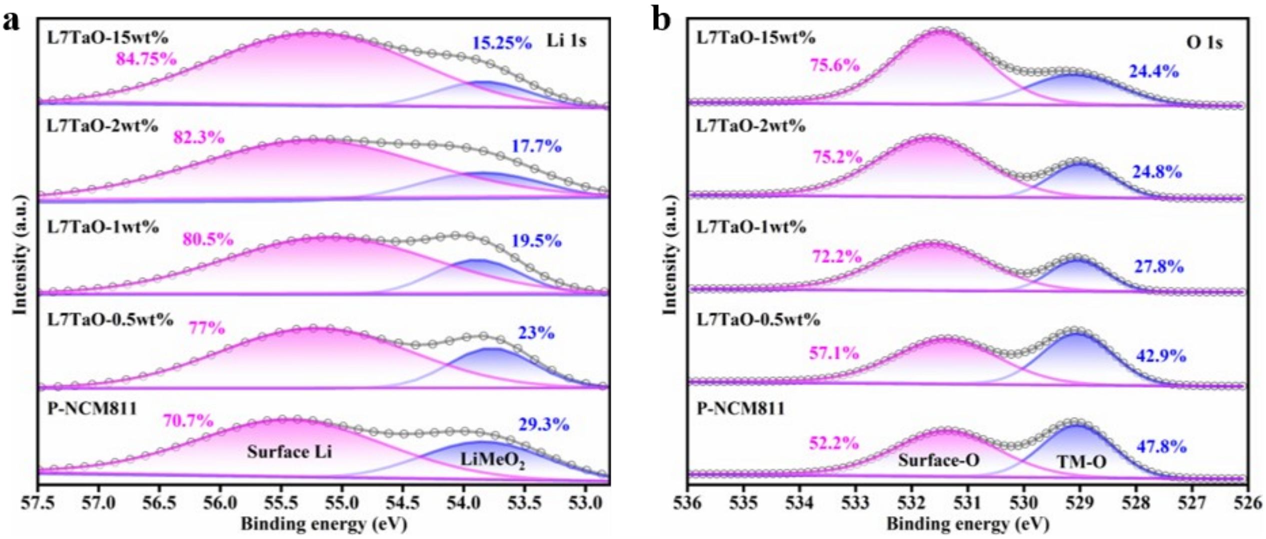

Fig. S8. (a) Li 1s and (b) O 1s XPS spectra of P-NCM811 and L7TaO-Q wt% (Q = 0.5, 1, 2 and 15) materials.

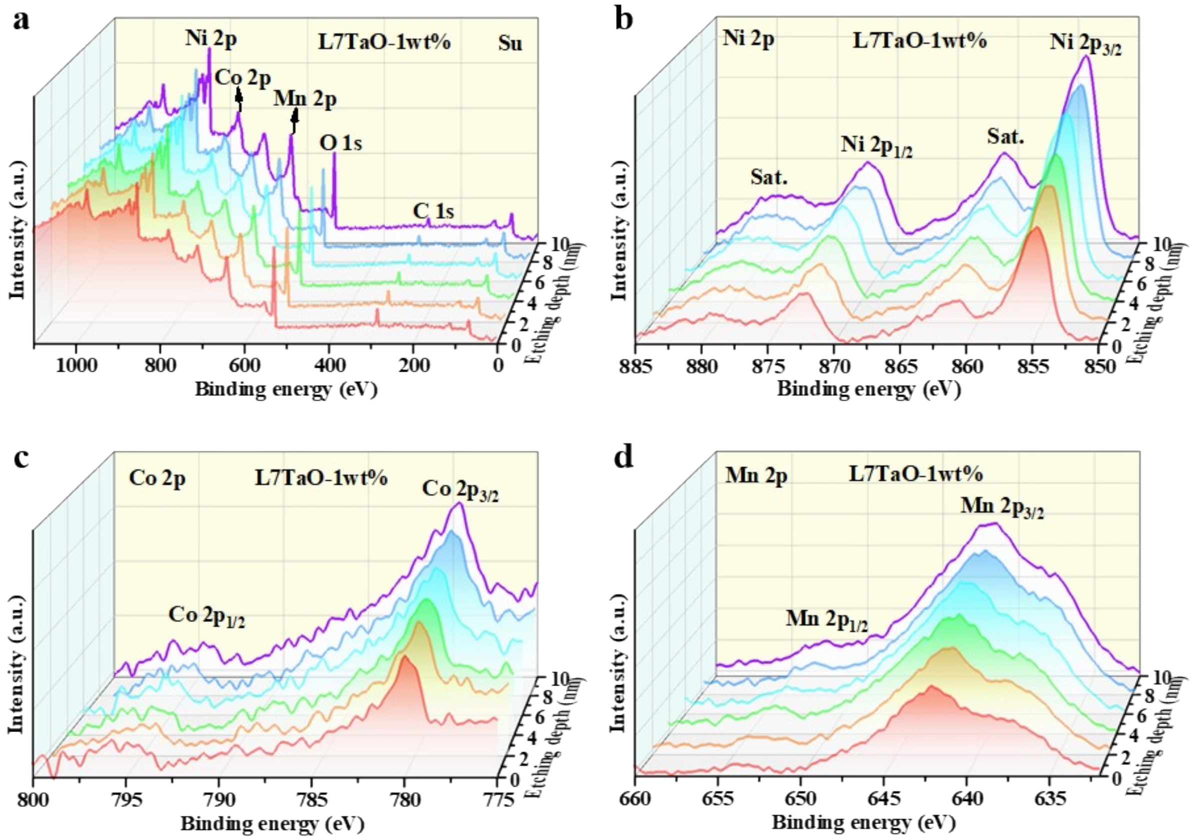

Fig. S9. XPS spectra evolution of (a) summary spectra, (b) Ni 2p, (c) Co 2p and (d) Mn 2p versus etching depth.

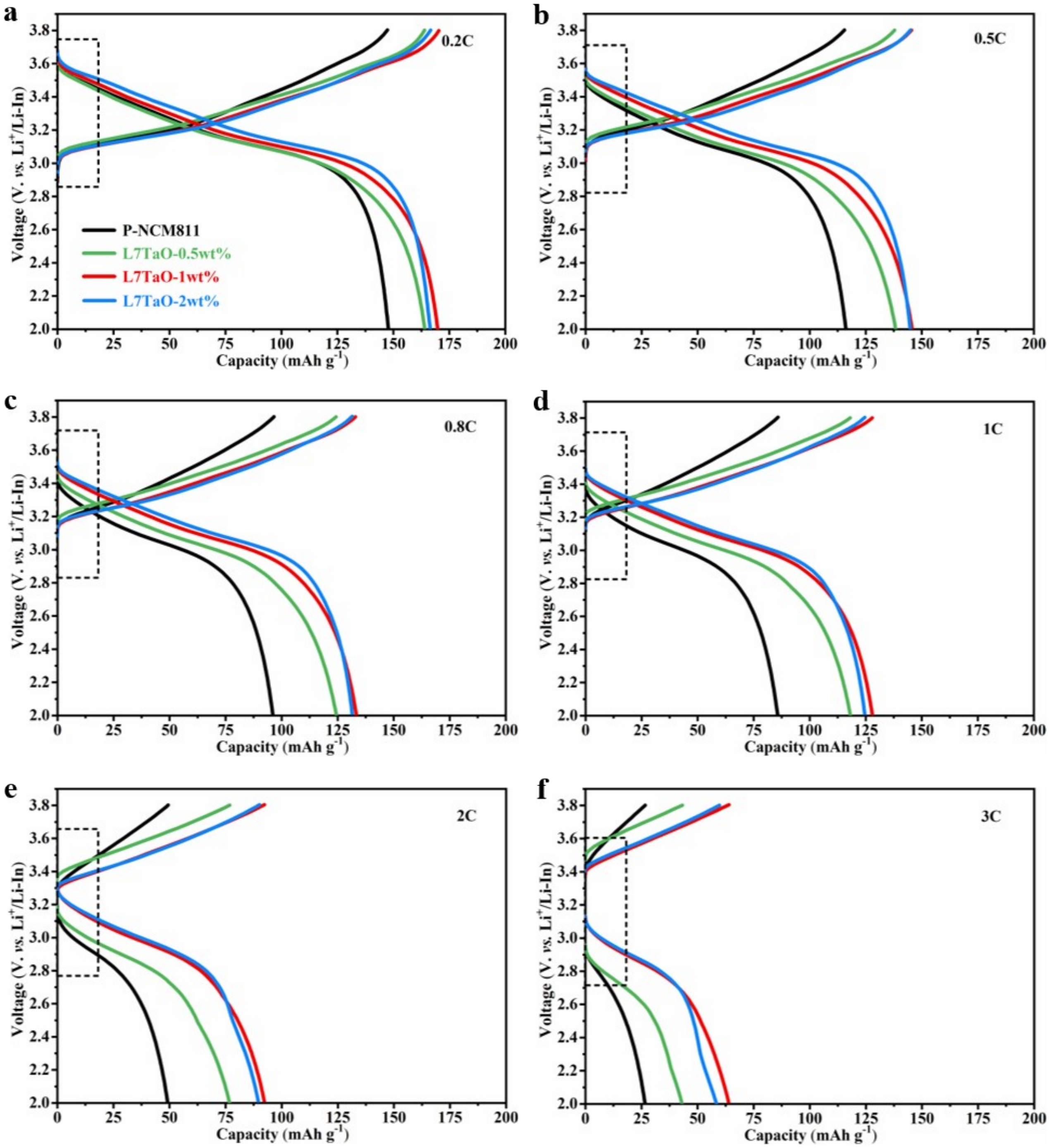

Fig. S10. Comparison of charge-discharge curves of the P-NCM811 and L7TaO-Q wt% (Q = 0.5, 1 and 2) at different current densities (1C = 170 mA g^{-1}), which clearly show the electrode polarization trends. (a) 0.2C, (b) 0.5C, (c) 0.8C, (d) 1C, (e) 2C and (f) 3C.

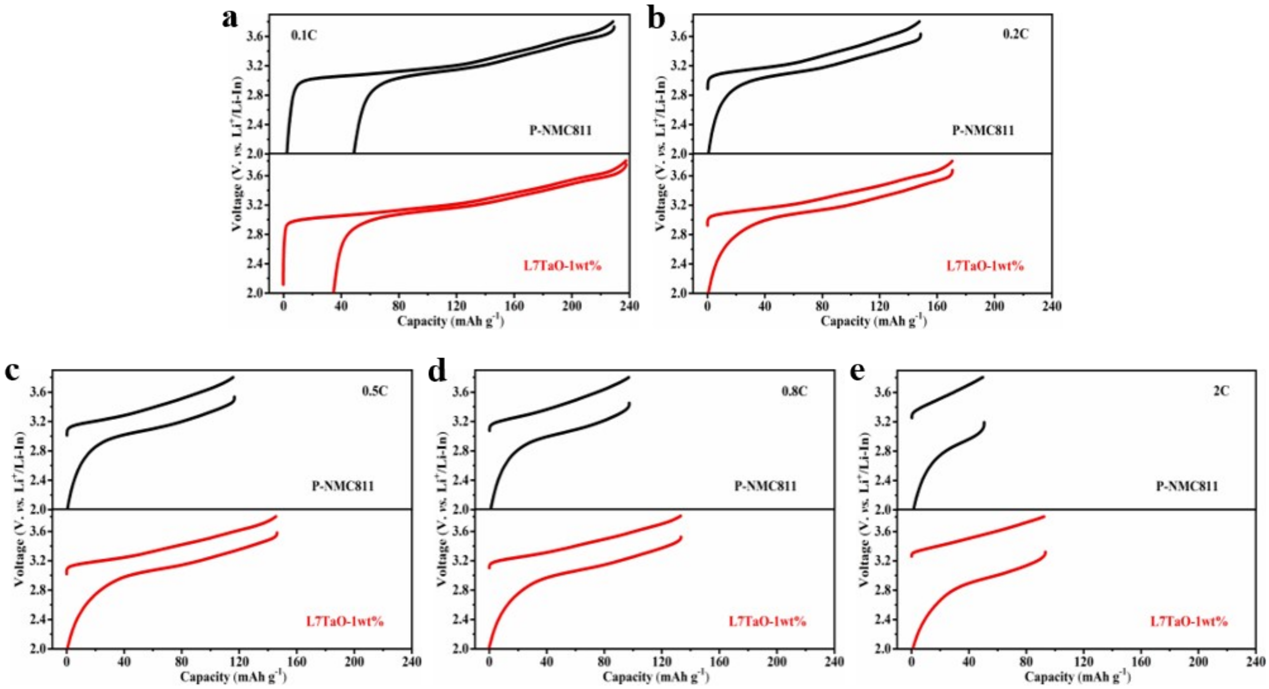

Fig. S11. Comparison of charge-discharge curves of the P-NCM811 and L7TaO-1 wt% at different current densities: (a) 0.1C, (b) 0.2C, (c) 0.5C, (d) 0.8C and (e) 2C. (1C = 170 mA g^{-1})

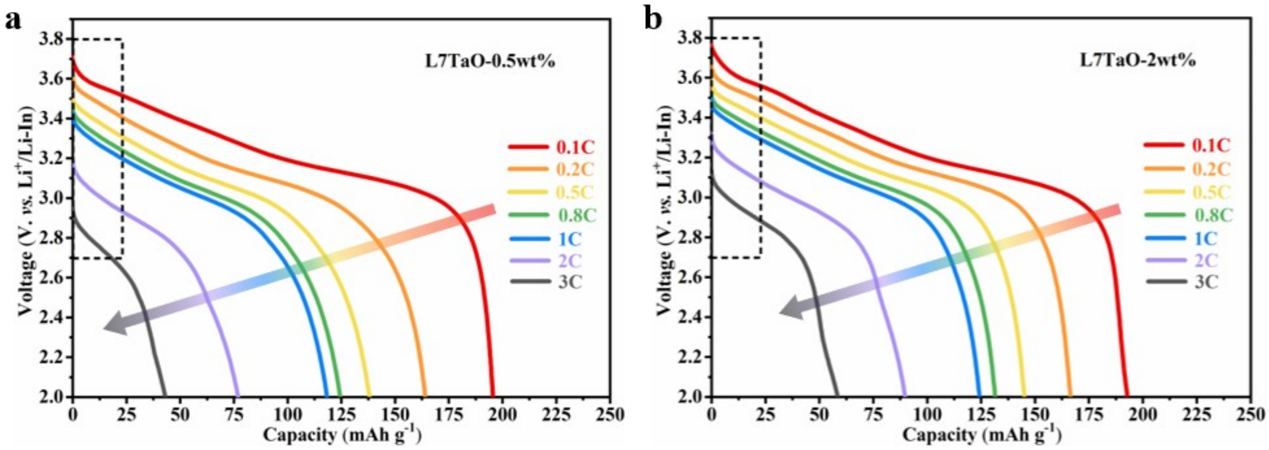

Fig. S12. The discharge curves of (a) L7TaO-0.5 wt% and (b) L7TaO-2 wt% under various current densities. (1C = 170 mA g^{-1})

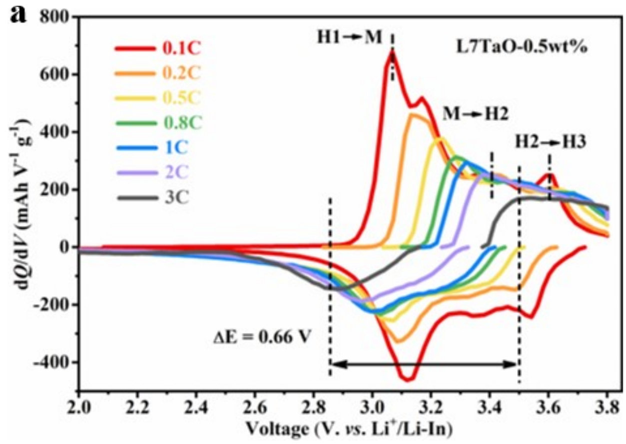

Fig. S13. The dQ/dV curves of (a) L7TaO-0.5 wt% and (b) L7TaO-2 wt% at different C-rates. (1C = 170 mA g^{-1})

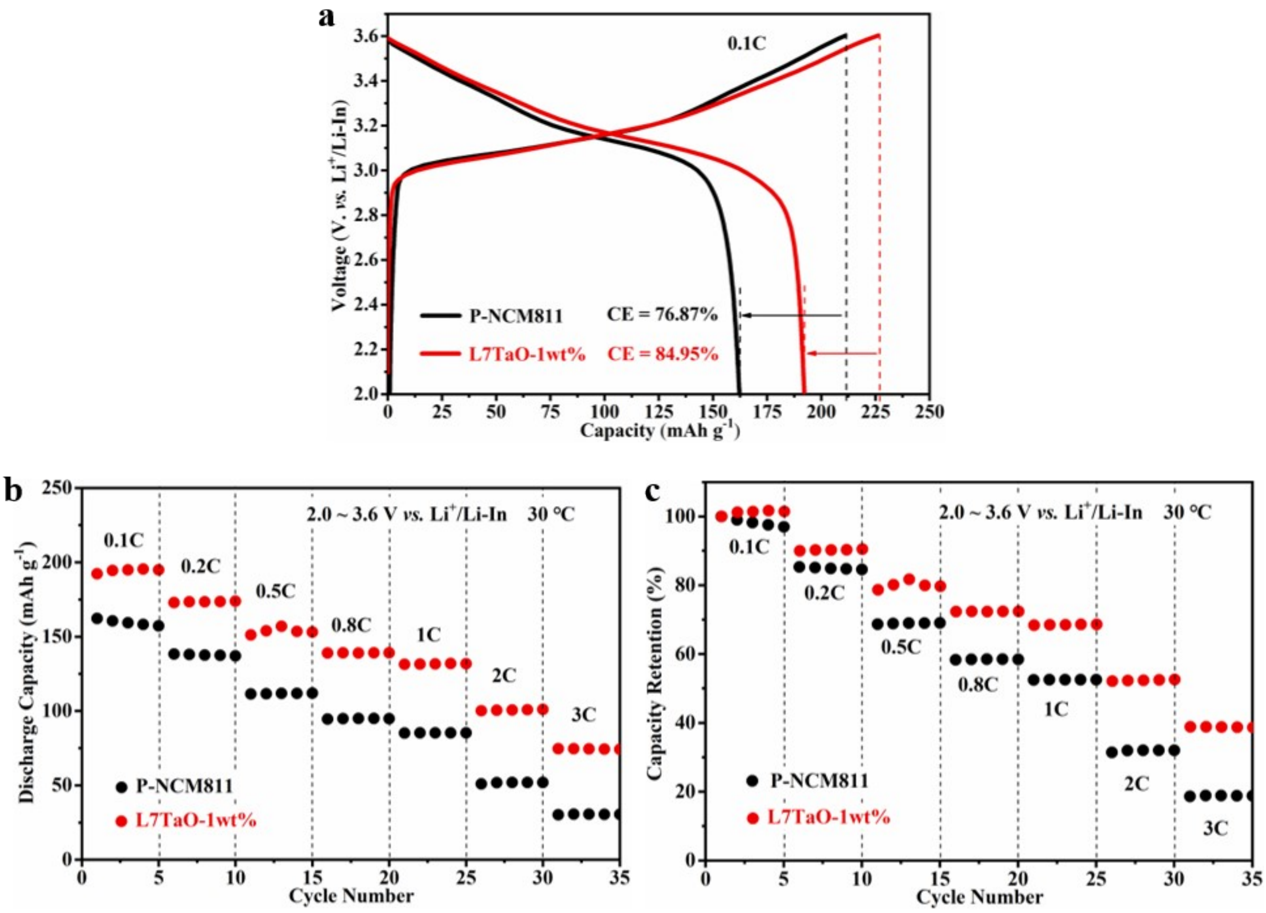

Fig. S14. Comparison of the electrochemical performance of P-NCM811 and L7TaO-1 wt% in ASSLBs at 2.0-3.6 V (*vs.* Li^+/Li-In) (30 °C). (a) The first charge-discharge profiles of the ASSLBs at 0.1C, and the initial Coulombic Efficiencies (CE). (b) Specific discharge capacities at different C-rates versus the cycle number (1C = 170 mA g^{-1}). (c) Capacity retentions curves at different C-rates.

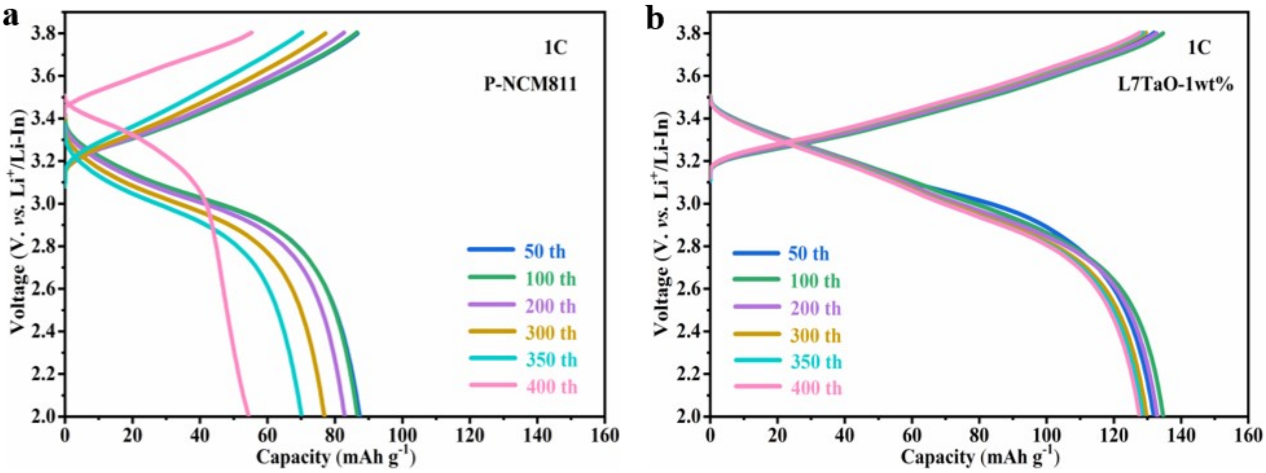

Fig. S15. Charge-discharge curves of (a) P-NCM811 and (b) L7TaO-1 wt% at 1 C in selected cycles, which clearly show the polarization trends.

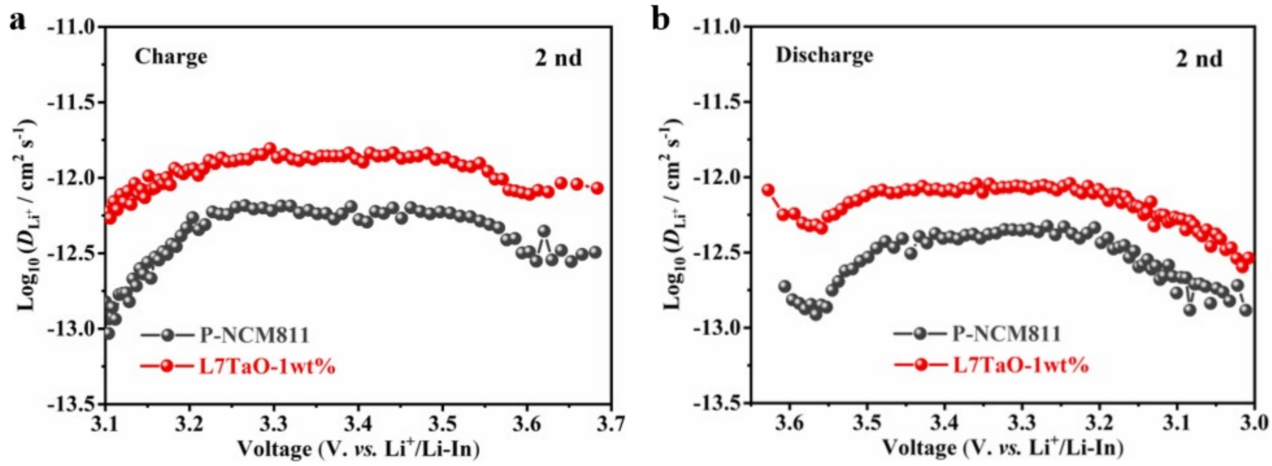

Fig. S16. Diffusion coefficients of Li^{+} ions calculated from the GITT curves as a function of voltage during the 2 nd (a) charge and (b) discharge process.

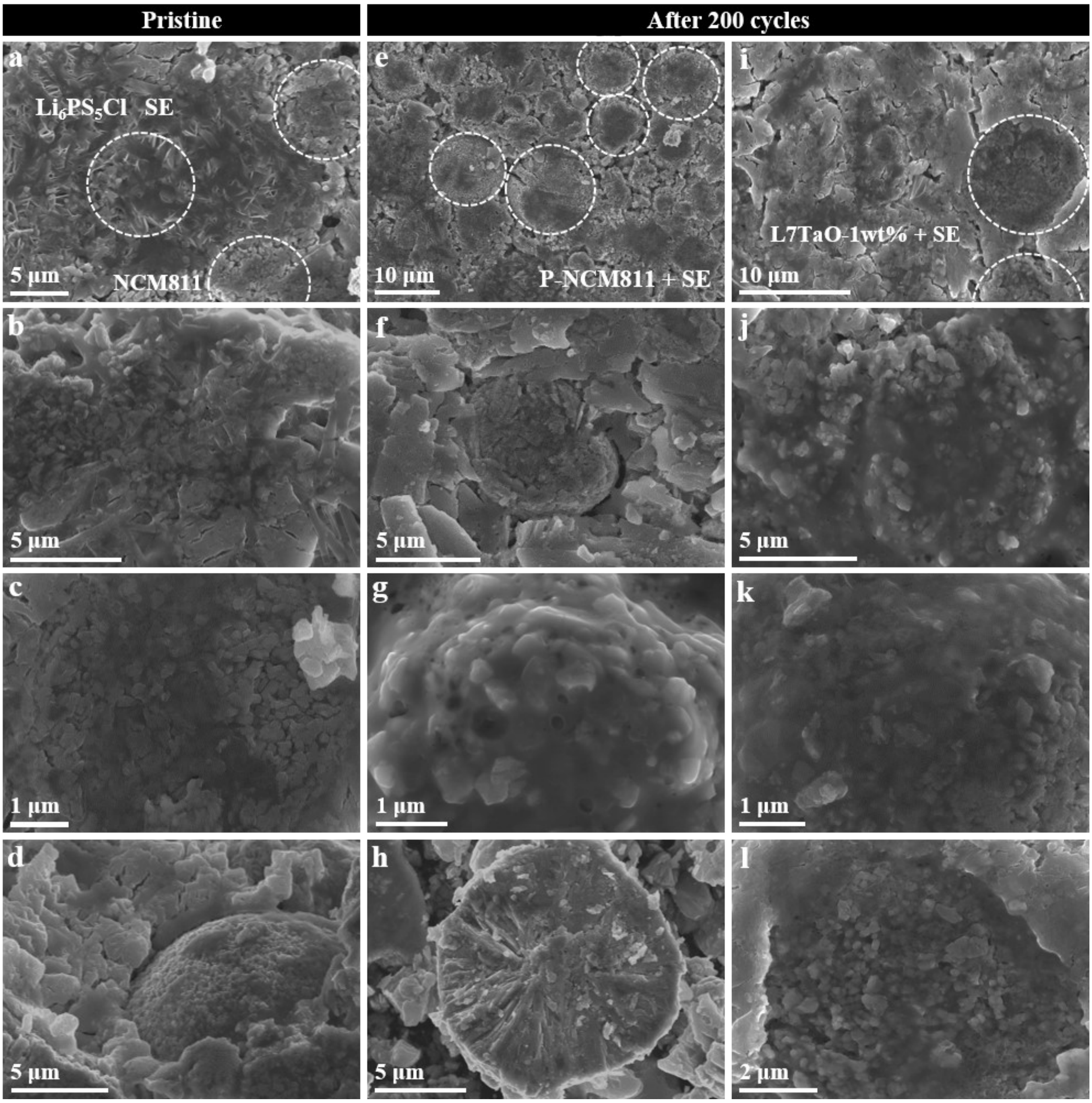

Fig. S17. SEM images at different magnifications of the cathode (a−d) in the pristine state and (e−l) after 200 cycles at 1C rate and 30 °C: (e−h) P-NCM811 and (i−l) L7TaO-1 wt%.

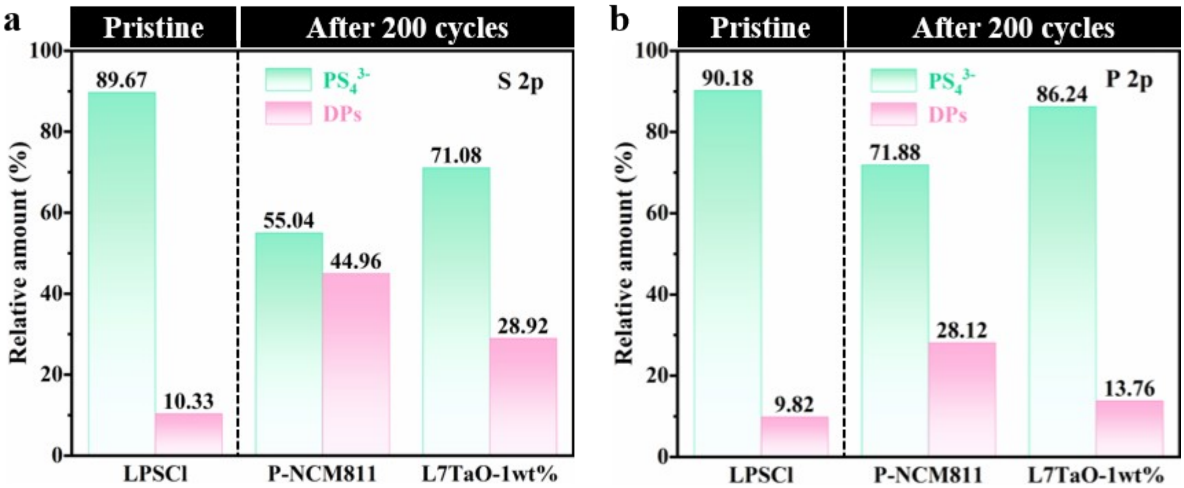

Fig. S18. Comparison of relative amounts of the S 2p/P 2p components for the cathodes after 200 cycles at 1C rate and 30 °C (see corresponding spectra in Fig. 7d, g) together with the pristine LPSCl as a reference.

Table S1. XRD Rietveld refinement results of P-NCM811 and L7TaO-Q wt% (Q = 0.5, 1, 2 and 15) materials.

Material	**Lattice parameter**			***c*/*a***	**R_p (%)**	**R_{wp} (%)**	**Ni^{2+} in Li^+ layer (%)**	**$I_{(003)}/I_{(104)}$**
	***a*[Å]**	***c*[Å]**	***V*[Å]**					
P-NCM811	2.87121	14.20076	101.385	4.94591	1.91	2.48	7.14	2.08318
L7TaO-0.5 wt%	2.86955	14.20179	101.275	4.94913	1.97	2.54	5.76	1.96489
L7TaO-1 wt%	2.86946	14.20385	101.283	4.95001	2.09	2.73	3.86	2.18367
L7TaO-2 wt%	2.86897	14.20432	101.252	4.95102	2.08	2.68	3.69	2.15563
L7TaO-15 wt%	2.86534	14.20569	100.934	4.95784	3.61	5.79	3.19	2.21828

Table S2. Simulated results for the Nyquist plots.

Cathode	R_s (Ω)		R_e (Ω)		R_{ct} (Ω)	
	Before	**After**	**Before**	**After**	**Before**	**After**
P-NCM811	29.52	33.98	1.12	1.26	28.10	53.01
L7TaO-1 wt%	28.07	28.71	1.00	1.56	19.47	25.47

Table S3. Li^+ diffusion coefficient D_{Li+} of P-NCM811 and L7TaO-1 wt% in the charge and discharge regions.

Cathode	D_{Li+} in the charge region/ cm^2 s^{-1}		D_{Li+} in the discharge region/ cm^2 s^{-1}	
	1 st	**2 nd**	**1 st**	**2 nd**
P-NCM811	7.29×10^{-13}	4.25×10^{-13}	4.19×10^{-13}	3.34×10^{-13}
L7TaO-1 wt%	1.28×10^{-12}	1.09×10^{-12}	9.76×10^{-13}	6.92×10^{-13}

Table S4. Summary comparison of electrochemical properties of our work with reported Ni-rich oxide cathodes in sulfide ASSLBs.

Ref.	Cathode	Coating	Sulfide solid electrolyte	Temperature & Voltage	Active material loading mass (mg cm^{-2})	Initial discharge capacity (mAh g^{-1}) & Coulombic efficiency	Cycle stability	Areal capacity (mAh cm^{-2})
Our work	**$LiNi_{0.8}Co_{0.1}Mn_{0.1}O_2$ (NCM811)**	**Li_7TaO_6**	**Li_6PS_5Cl**	**30°C & 2.0-3.8 (V *vs.* Li^+/Li-In)**	**8.92**	**203 (0.1C) & 85.4%**	**134.7 mAh g^{-1} & 102.6% (1C, 100 cycles); 123.9 mAh g^{-1} & 94.4% (1C, 500 cycles); 114.3 mAh g^{-1} & 87.1% (1C, 1000 cycles); 94.5 mAh g^{-1} & 72% (1C, 2000 cycles); 85.8 mAh g^{-1} & 65.4% (1C, 3000 cycles); 85.1 mAh g^{-1} & 64.8% (1C, 4000 cycles); 84.3 mAh g^{-1} & 64.2% (1C, 5000 cycles); 80.2 mAh g^{-1} & 61.1% (1C, 5650 cycles).**	**1.52 (1C)**
[1]	NCM811	$LiNbO_3$	Li_6PS_5Cl	30°C & 2.5-4.0 (V *vs.* Li^+/Li)	4.00	111.7 (0.05C) & 66.8%	100.2 mAh g^{-1} & 89.7% (0.05C, 100 cycles)	0.80 (1C)
[2]	NCM811	LiOH	Li_6PS_5Cl	25°C & 2.5-4.2 (V *vs.* Li^+/Li-In)	5.53	158.9 (0.1C) & ~ 64%	~ 130 mAh g^{-1} & 90% (0.1C, 600 cycles)	1.10 (1C)
[3]	NCM811	No coating (clean surface)	$Li_{5.5}PS_{4.5}Cl_{1.5}$	25°C & 2.1-3.8 (V *vs.* Li^+/Li-In)	8.92	156.8 (0.05C) & 76%	108.6 mAh g^{-1} & 87.7% (0.2C, 200 cycles)	n.a.
[4]	NCM811	$LiCoO_2$-$LiNbO_3$	$Li_{10}GeP_2S_{12}$	35°C & 2.1-3.78 (V *vs.* Li^+/Li-In)	10.23	182.4 (0.1C) & n.a.	~ 128 mAh g^{-1} & 80% (0.3C, 585 cycles)	2.05 (1C)

[5]	NCM811	$LiNbO_3$	$Li_{10}GeP_2S_{12}$	35°C & 2.1-3.78 (V *vs.* Li^+/Li-In)	10.23	162 (0.1C) & 85.9%	~ 105 mAh g^{-1} & 77.9% (0.5C, 50 cycles)	2.05 (1C)
[6]	NCM811	Li_3PO_4	$Li_{10}GeP_2S_{12}$	25°C & 2.1-3.9 (V *vs.* Li^+/Li-In)	8.92	170.6 (0.1C) & 75.1%	96.1 mAh g^{-1} & 58.9% (0.2C, 300 cycles)	n.a.
[7]	$LiNi_{0.88}Co_{0.09}Mn_{0.03}O_2$	N_2/CS_2 sulfide layer	Li_6PS_5Cl	33°C & 1.5-2.8 (V *vs.* Li^+/LTO)	1.27	200.7 (0.1C) & 77.7%	131.2 mAh g^{-1} & 87% (1C, 500 cycles)	0.25 (1C)
[8]	$LiNi_{0.85}Co_{0.10}Mn_{0.05}O_2$	ZrO_2	Li_6PS_5Cl	45°C & 1.35-2.75 (V *vs.* Li^+/LTO)	11.30	204 (0.1C) & 89%	156 mAh g^{-1} & 83% (0.2C, 160 cycles)	2.15 (1C)
[9]	$LiNi_{0.85}Co_{0.10}Mn_{0.05}O_2$	HfO_2	Li_6PS_5Cl	45°C & 1.4-2.8 (V *vs.* Li^+/LTO)	10.55	200 (0.1C) & 87.8%	139.4 mAh g^{-1} & 82% (0.5C, 70 cycles)	2.00 (1C)
[10]	$LiNi_{0.82}Co_{0.12}Mn_{0.06}O_2$	$LiTaO_3$	Li_6PS_5Cl	30°C & 1.9-3.7 (V *vs.* Li^+/Li-In)	5.97	202.1 (0.05C) & 72.4%	~ 167.7 mAh g^{-1} & 83% (0.2C, 30 cycles) (1.9-3.9 V *vs.* Li^+/Li-In))	1.01 (1C)
[11]	$Li(Ni_{0.9}Co_{0.05}Mn_{0.05})_{0.8}Co_{0.2}O_2$	Al_2O_3-$LiAlO_2$	$Li_{9.54}Si_{1.7}P_{1.44}S_{11.7}Cl_{0.3}$	45°C & 2.1-3.68 (V *vs.* Li^+/Li-In)	36.94	158.6 (0.2C) & 88.3%	136.75 mAh g^{-1} & 96.3% (1C, 500 cycles)	7.39 (1C)
[12]	$LiNi_{0.70}Co_{0.15}Mn_{0.15}O_2$ (NCM701515)	Al_2O_3-$LiAlO_2$	Li_6PS_5Cl	25°C & 2.0-3.7 (V *vs.* Li^+/Li-In)	10.39	154 (0.1C) & 70.4%	75 mAh g^{-1} & 54% (0.25C, 100 cycles)	2.08 (1C)
[13]	NCM701515	$Li_4Ti_5O_{12}$	Li_6PS_5Cl	25°C & 2.0-3.7 (V *vs.* Li^+/Li-In)	10.39	135 (0.1C) & 70.4%	64.8 mAh g^{-1} & 48% (0.25C, 100 cycles)	2.08 (1C)
[14]	$LiNi_{0.6}Co_{0.2}Mn_{0.2}O_2$ (NCM622)	Li_2CO_3-$LiNbO_3$	Li_6PS_5Cl	45°C & 1.35-2.85 (V *vs.* Li^+/LTO)	8.92	180 (0.2C) & 90%	82 mAh g^{-1} & 45.5% (0.2C, 200 cycles)	1.61 (1C)
[15]	NCM622	$Li_{0.35}La_{0.55}TiO_3$	Li_6PS_5Cl	25°C & 2.2-3.7 (V *vs.* Li^+/Li-In)	6.40	179.9 (0.05C) & 78.1%	152.1 mAh g^{-1} & 84.5% (0.1C, 100 cycles)	1.28 (1C)

[16]	NCM622	$LiZr_2(PO_4)_3$	Li_6PS_5Cl	30℃ & 2.0-3.7 (V *vs.* Li^+/Li-In)	8.92	145.6 (0.1C) & 79.4%.	117.4 mAh g^{-1} & 86.2% (0.2C, 100 cycles)	n.a.
[17]	NCM622	$TiNb_2O_7$	$Li_{10}GeP_2S_{12}$	30℃ & 2.1-3.8 (V *vs.* Li^+/Li-In)	9.91	180.3 (0.05C) & 86.3%	~ 145 mAh g^{-1} & 92.2% (0.1C, 140 cycles)	1.78 (1C)
[18]	NCM622	$Li_{1.4}Al_{0.4}Ti_{1.6}(PO_4)_3$	$Li_{10}SnP_2S_{12}$	25℃ & 2.2-3.7 (V *vs.* Li^+/Li-In)	7.13	152.1 (0.05C) & 86.4%	147.8 mAh g^{-1} & 87.6% (0.1C, 100 cycles)	n.a.
[19]	NCM622	$LiNbO_3$	$Li_{9.54}Si_{1.7}P_{1.44}S_{11.7}Cl_{0.3}$	40℃ & 2.1-3.68 (V *vs.* Li^+/Li-In)	10.23	175.7 (0.1C) & 88.7%.	147 mAh g^{-1} & 91.3% (0.5C, 100 cycles)	2.05 (1C)
[20]	NCM622	$LiNbO_3$-Li_2CO_3	β-Li_3PS_4	25℃ & 1.35-2.85 (V *vs.* Li^+/LTO)	8.92	136 (0.1C) & 87%	~ 125 mAh g^{-1} & 91% (0.1C, 100 cycles)	1.61 (1C)
[21]	NCM622	Li_2CuO_2-CuO	$Li_7P_2S_8I$	25℃ & 2.38-3.68 (V *vs.* Li^+/Li-In)	n.a.	123 (0.05C) & n.a.	105. mAh g^{-1} & 86% (0.05C, 20 cycles)	n.a
[22]	NCM622	$LiNbO_3$	$Li_7P_2S_8I$	25℃ & 2.38-3.68 (V *vs.* Li^+/Li-In)	n.a.	135.1 (0.1C) & n.a.	~120 mAh g^{-1} & 84.4% (0.1C, 20 cycles)	n.a

References

[1] J. Zhang, H. Zhong, C. Zheng, Y. Xia, C. Liang, H. Huang, Y. Gan, X. Tao and W. Zhang, *J. Power Sources*, 2018, **391**, 73.

[2] Y. Zhang, X. Sun, D. Cao, G. Gao, Z. Yang, H. Zhu and Y. Wang, *Energy Storage Mater.*, 2021, **41**, 505.

[3] S. Deng, Q. Sun, M. Li, K. Adair, C. Yu, J. Li, W. Li, J. Fu, X. Li, R. Li, Y. Hu, N. Chen, H. Huang, L. Zhang, S. Zhao, S. Lu and X. Sun, *Energy Storage Mater.*, 2021, **35**, 661.

[4] X. Li, Q. Sun, Z. Wang, D. Song and L. Zhu, *J. Power Sources*, 2020, **456**, 227997.

[5] X. Li, L. Jin, D. Song, H. Zhang, X. Shi, Z. Wang, L. Zhang and L. Zhu, *J. Energy Chem.*, 2020, **40**, 39.

[6] S. Deng, X. Li, Z. Ren, W. Li, J. Luo, J. Liang, J. Liang, M. N. Banis, M. Li, Y. Zhao, X. Li, C. Wang, Y. Sun, Q. Sun, R. Li, Y. Hu, H. Huang, L. Zhang, S. Lu, J. Luo and X. Sun, *Energy Storage Mater.*, 2020, **27**, 117.

[7] Y. Wang, Z. Wang, D. Wu, Q. Niu, P. Lu, T. Ma, Y. Su, L. Chen, H. Li and F. Wu, *eScience*, 2022.

[8] Y. Ma, J. H. Teo, F. Walther, Y. Ma, R. Zhang, A. Mazilkin, Y. Tang, D. Goonetilleke, J. Janek, M. Bianchini and T. Brezesinski, *Adv. Funct. Mater.*, 2022, **32**, 2111829.

[9] D. Kitsche, Y. Tang, Y. Ma, D. Goonetilleke, J. Sann, F. Walther, M. Bianchini, J. Janek and T. Brezesinski, *ACS Applied Energy Materials*, 2021, **4**, 7338.

[10] J. S. Lee and Y. J. Park, *ACS Appl. Mater. Interfaces,* 2021, **13**, 38333.

[11] X. Li, Y. Sun, Z. Wang, X. Wang, H. Zhang, D. Song, L. Zhang and L. Zhu, *Electrochim. Acta*, 2021, **391**, 138917.

[12] R. S. Negi, Y. Yusim, R. Pan, S. Ahmed, K. Volz, R. Takata, F. Schmidt, A. Henss and M. T. Elm, *Adv. Mater. Interfaces*. 2022, **9**, 2101428.

[13] R. S. Negi, P. Minnmann, R. Pan, S. Ahmed, M. J. Herzog, K. Volz, R. Takata, F. Schmidt, J.

Janek and M. T. Elm, *Chem. Mater.*, 2021, **33**, 6713.

[14] F. Walther, F. Strauss, X. Wu, B. Mogwitz, J. Hertle, J. Sann, M. Rohnke, T. Brezesinski and J. Janek, *Chem. Mater.*, 2021, **33**, 2110.

[15] Z. Fan, J. Xiang, Q. Yu, X. Wu, M. Li, X. Wang, X. Xia and J. Tu, *ACS Appl. Mater. Interfaces*, 2022, **14**, 726.

[16] X. Sun, L. Wang, J. Ma, X. Yu, S. Zhang, X. Zhou and G. Cui, *ACS Appl. Mater. Interfaces*, 2022, **14**, 17674.

[17] N. Sun, Y. Song, Q. Liu, W. Zhao, F. Zhang, L. Ren, M. Chen, Z. Zhou, Z. Xu, S. Lou, F. Kong, J. Wang, Y. Tong and J. Wang, *Adv. Energy Mater.*, 2022, 2200682.

[18] X. Li, Z. Jiang, D. Cai, X. Wang, X. Xia, C. Gu and J. Tu, *Small*, 2021, **17**, 2103830.

[19] X. Li, W. Peng, R. Tian, D. Song, Z. Wang, H. Zhang, L. Zhu and L. Zhang, *Electrochim. Acta*, 2020, **363**, 137185.

[20] A. Y. Kim, F. Strauss, T. Bartsch, J. H. Teo, T. Hatsukade, A. Mazilkin, J. Janek, P. Hartmann and T. Brezesinski, *Chem. Mater.*, 2019, **31**, 9664.

[21] S. Jung, R. Rajagopal and K. Ryu, *Mater. Chem. Phys.*, 2021, **270**, 124808.

[22] Y. Kim, R. Rajagopal, S. Kang and K. Ryu, *Chem. Eng. J.*, 2020, **386**, 123975.